Reduced-Order Pulse-Motor Ignition Control Logic

V.H.L. Cheng*
NASA Ames Research Center, Moffett Field, California
and
P.K.A. Menon†
Georgia Institute of Technology, Atlanta, Georgia
and
N.K. Gupta‡ and M.M. Briggs§
Integrated Systems, Santa Clara, California

The higher total impulse and energy management potential available in a pulse motor can be exploited with optimal guidance and propulsion control methods to improve missile performance. Under the assumptions of same propellant formulation and similar grain configuration of the pulses, a pulse motor can generally deliver higher specific impulse than its boost-sustain counterpart, leading to higher total impulse with the same launch weight despite a weight penalty on the pulse motor due to barrier insulation and an additional igniter; moreover, the pulse motor also allows arbitrary pulse delays between pulses. To fully exploit such energy management capabilities requires a real-time on-board pulse ignition controller. This paper studies the pulse ignition problem for a generic medium-range air-to-air missile from an optimal control viewpoint, using a minimum flight-time performance index. To make real-time mechanization feasible with state-of-the-art microprocessors, the optimal control solution is reduced to an implementable algorithm using singular-perturbation arguments and engineering approximations for the midcourse guidance problem. The resulting ignition control used in conjunction with the midcourse guidance law is then shown to command pulse ignition within the desirable period, leading to significant performance improvement over the boost-sustain motor.

I. Introduction

THIS paper studies the application of pulse motors in tactical missiles. Specifically, the medium-range air-to-air missiles (MRAAM's) are considered as their missions require prudent energy management.

Conventional MRAAM concepts use boost-sustain motors for propulsion. Except for close-in engagements, the missile's radar seeker will not acquire the target at launch. For guidance purposes, the midcourse phase of the flight is defined as the period following launch until seeker lock-on is realized; the remaining terminal phase is for homing guidance. Conventional MRAAM's use proportional navigation (pronav) or a variation thereof for terminal guidance, with additional preprogrammed g-bias commands in the midcourse phase to fly the missile at higher altitudes for lower drag. Under typical standoff-launch conditions, the boost-sustain motor burns out in the midcourse phase.

For more effective energy management against standoff targets, optimal control methods have been applied to the midcourse flight regime to maximize MRAAM performance. Reference 1 describes an advanced midcourse guidance law obtained by the application of singular-perturbation techniques to reduce the order of the optimal control problem, with additional approximations to simplify the adjoint equations. The resulting guidance algorithm is sufficiently simple for on-board implementation, and has led to large overall performance improvement of the missile. The application of the singular-perturbation techniques for missile guidance has been discussed earlier by Sridhar and Gupta.[2] More recently, on-line aircraft flight-path control using this technique has been investigated by Calise et al.[3,4]

Recent developments in solid-propellant rocket propulsion have established the pulse motor as a viable alternative to the conventional boost-sustain motor for MRAAM's. For a two-pulse motor, the pulses can be ignited separately, with a variable delay for ignition of the second pulse. This is achieved at the cost of an additional igniter and thermal barrier material. A solid-propellant pulse motor can be designed to burn the propellant in all of its pulses at about the same chamber pressure, given due regard for the effect of nozzle throat erosion upon chamber pressure. Assuming that the same propellant formulation and similar grain configuration are used in each of the pulses, the delivered specific impulse at standard conditions varies only slightly from pulse to pulse; therefore, the average delivered specific impulse is only slightly less than that of the first pulse, regardless of the pulse delay time. Whereas a boost-sustain rocket motor with more than 2-to-1 boost-to-sustain thrust ratio sacrifices specific impulse with its lower sustain chamber pressure associated with its fixed nozzle design, the pulse motor generally delivers a significantly higher average specific impulse than a boost-sustain motor of comparable dimension and mass. Although pulse motors require slightly more inert consumable weight than boost-sustain motors in the form of thermal barrier and multiple-igniter charge material, the pulse motor can retain a 5–7% sea-level total delivered impulse advantage over its boost-sustain counterpart at fixed gross weight.

Another advantage of a pulse motor is the freedom to control the firing time of the second and subsequent pulses, whereas the thrust profile of a boost-sustain motor is contiguous and predetermined. To fully exploit such advantage, the second pulse should be ignited at an instant that optimizes

Presented as Paper 85-0500 at the AIAA 23rd Aerospace Sciences Meeting, Reno, NV, Jan. 14–17, 1985; received Feb. 19, 1985; revision received Aug. 6, 1986.

*Research Scientist, formerly Senior Research Scientist of Integrated Systems, Inc.
†Associate Professor, formerly Research Scientist of Integrated Systems, Inc. Member AIAA.
‡President. Member AIAA.
§Manager, Missile Division. Associate Fellow AIAA.

missile performance. Given a performance index, it is immediately obvious that the optimal pulse-motor ignition control is dependent on the particular flight trajectory dictated by the guidance scheme. Consequently, pulse-motor ignition control is tightly coupled with the guidance function and the two should be developed simultaneously using the same performance index. It should be pointed out that since the pulse duration is not a variable, we are not free to alter the thrust profile of the motor pulses; hence, a given pulse motor cannot be considered a superset of the boost-sustain motor, and there is no guarantee that the pulse motor can outperform the boost-sustain motor under all conditions despite its aforementioned advantages.

We formulate the optimal guidance and ignition control problem as a minimum flight-time problem. We adopt the same framework as in Ref. 1, viz., the optimal control problem is re-examined at every sample instant throughout the flight, and the resulting control is commanded until the next sample instant. Such real-time feedback of the engagement conditions allows the missile to adapt to the changing engagement geometry. Further, note that this approach permits the treatment of the missile guidance task as a one-sided optimal control problem rather than as a pursuit-evasion problem.[5] The pulse-motor ignition control problem is discussed in Sec. II, which results in the implementation algorithm of Sec. III. The ignition control algorithm is validated using computer simulations in Sec. IV, which also compares the performance of the pulse motor controlled by such algorithm to that of a baseline boost-sustain motor. Section V concludes with a summary of the pulse-motor performance.

II. Pulse-Motor Ignition Control

In this section, MRAAM's with pulse-motor propulsion consisting of two boost pulses are considered. The missile is launched upon ignition of the first pulse. The guidance and pulse-motor ignition control is studied as an integral problem. For MRAAM's, this problem calls for the consideration of the midcourse flight regime.

During the midcourse flight, the MRAAM depends on periodic updates of target information from the launch aircraft or other tracking platforms. To enhance intercept performance against maneuvering targets, the missile guidance and pulse-motor control scheme is repeated at each sample instant using the latest available information about the target and missile states. This completes the midcourse guidance and control loop. Since direct measurement of target maneuver information during midcourse is not available, the missile's dependence on in-flight target updates to adapt its own trajectory in a feedback manner is crucial to guarantee target interception. This reduces the need to make at-best unjustified assumptions on the target's future maneuver tactics.

Remark: For short-range missions not considered here, knowledge of target state and maneuver tactics can serve to reduce miss distance. Reference 6 contains a homing guidance law based on simplification of the short-range optimal guidance problem by singular-perturbation considerations, which explicitly models the target maneuvering in a coordinated turn.

Missile Model

The missile model considered herein is identical to that of Ref. 1: specifically, the state variables are 1) the missile position coordinates x, y, and h in a Cartesian inertial frame, where h represents altitude; 2) the specific energy [$E = h + v^2/(2g)$, where v denotes the missile speed]; and 3) the flight-path angle γ and heading angle ϕ (see Fig. 1). In the formulation, it is assumed that the missile is launched at time $t = 0$. At sample instant $t = t_0 \geq 0$, the problem with initial time t_0 and a free but optimal terminal time t_f is studied. Observe that the optimal terminal time t_f, corresponding to different initial time t_0, may be different, leading to a real-time feedback guidance law. The state equations describing the missile dynamics are

$$\dot{x} = v\cos\gamma\cos\phi, \quad x(t_0) = x_0 \tag{1}$$

$$\dot{y} = v\cos\gamma\sin\phi, \quad y(t_0) = y_0 \tag{2}$$

$$\dot{h} = v\sin\gamma, \quad h(t_0) = h_0 \tag{3}$$

$$\dot{E} = \frac{v(T-D)}{mg}, \quad E(t_0) = E_0 \tag{4}$$

$$\dot{\phi} = \frac{a\sin\sigma}{v\cos\gamma}, \quad \phi(t_0) = \phi_0 \tag{5}$$

$$\dot{\gamma} = \frac{a\cos\sigma - g\cos\gamma}{v}, \quad \gamma(t_0) = \gamma_0 \tag{6}$$

where T is the motor thrust, m the missile mass, a the lift acceleration magnitude, σ the lift orientation, relative to vertical plane through the velocity vector, and D the drag. Observe that the thrust component normal to the velocity vector is ignored in this model for medium-range launches, and the lift vector is always normal to the velocity vector. The drag is expressed as

$$D = qsC_D = qs(C_{D_0} + C_{D_\alpha}|\alpha_T| + C_{D_{\alpha^2}}\alpha_T^2) \tag{7}$$

where C_D is the total drag coefficient including the zero-lift drag coefficient C_{D_0} and the induced-drag coefficients C_{D_α} and $C_{D_{\alpha^2}}$, q is the dynamic pressure ($=\frac{1}{2}\rho v^2$), ρ the air density, given as a function of altitude, s the missile reference area, and α_T the total angle of attack. The total angle of attack is related to the lift force through

$$\text{lift} = qsC_{L_\alpha}\alpha_T \tag{8}$$

where C_{L_α} is the lift-coefficient slope with respect to α_T.

The target state is not considered directly in the state equations. The in-flight available target state is used instead to predict a point of intercept by the algorithm presented in Sec. III. This predicted intercept point is treated as a terminal condition for the system (1–6), and a minimum flight-time solution is sought. It is readily observed that using the predicted point of intercept as a terminal condition is only a matter of convenience and simplification, as the target may not arrive at that point in space exactly at the same time as the minimum flight-time solution. Consequently, any reasonable method of prediction can be used. For our study, the intercept point as predicted during midcourse is based on assuming a constant-velocity target and a constant-speed missile. Note further that the time associated with the point of intercept prediction is not used by the formulation. The terminal condition can thus be identified as

$$(x, y, h)(t_f) = (x_f, y_f, h_f) \tag{9}$$

The thrust of the pulse motor is modeled by two rectangular pulses with magnitudes T_1 and T_2 and durations τ_{p1} and τ_{p2}, respectively. The first pulse initiates at $t = 0$, and there is a variable coast time τ_c between the two pulses (Fig. 2). Hence,

$$T(t) = T_1[\mathcal{H}(t) - \mathcal{H}(t-\tau_{p1})] + T_2[\mathcal{H}(t-\tau_c-\tau_{p1}) - \mathcal{H}(t-\tau_{p2}-\tau_c-\tau_{p1})], \quad t\in\mathbb{R} \tag{10}$$

where $\mathcal{H}$: $\mathbb{R}\to\mathbb{R}$ is the (Heaviside) unit step function.

The mass of the missile can be conveniently modeled such that the mass-flow rate is a monotonically increasing function of thrust amplitude passing through the origin, i.e., a monotonically increasing function f: $\mathbb{R}_+ \to \mathbb{R}_+$ exists such that

$$-\dot{m}(t) = f(T(t)), \quad f(0) = 0 \tag{11}$$

Hence,

$$m(t) = \begin{cases} m_0 - k_1 t, & 0 \le t \le \tau_{p1} \\ m_0 - k_1 \tau_{p1}, & \tau_{p1} \le t \le \tau_c + \tau_{p1} \\ m_0 - k_1 \tau_{p1} - k_2(t - \tau_c - \tau_{p1}), & \tau_c + \tau_{p1} \le t \le \tau_{p2} + \tau_c + \tau_{p1} \\ m_0 - k_1 \tau_{p1} - k_2 \tau_{p2}, & \tau_{p2} + \tau_c + \tau_{p1} \le t \end{cases} \tag{12}$$

where $k_1 = f(T_1)$ and $k_2 = f(T_2)$.

Control Variables

The control variables for the missile model [Eqs. (1–12)] are:

1) a: $[t_0, t_f] \to \mathbb{R}_+$, the commanded missile lift acceleration, which is assumed to be equal to the actual lift acceleration since the autopilot has a much faster time constant than the missile state dynamics.

2) σ: $[t_0, t_f] \to (-\pi, \pi)$, the lift orientation.

3) $\tau_c \in \mathbb{R}_+$, the interpulse coast duration as defined previously.

Functionally, the optimal values of a and σ constitute the guidance law and τ_c defines the pulse-motor ignition control.

Optimal Control Problem

The minimum flight-time optimal control problem is to determine the controls a, σ, and τ_c by minimizing the cost function J

$$J = t_f - t_0 = \int_{t_0}^{t_f} \mathrm{d}t \tag{13}$$

where t_f is free, subject to the dynamic constraints of Eqs. (1–12), including the initial and final conditions. This performance index is equivalent to a maximum f-pole, which is a performance criterion affecting launch aircraft vulnerability to attack. (The f-pole is defined as the minimum distance between the launch aircraft and the target over the flight time of the launched missile.)

Optimal Control Solution: Two-Point Boundary-Value Problem

The solution to the optimal control problem is obtained by defining the variational Hamiltonian[7] as

$$H = \lambda_\xi^T \dot{\xi} + 1 \tag{14}$$

where $\xi = (x, y, h, E, \phi, \gamma)^T$ and $\lambda_\xi = (\lambda_x, \lambda_y, \lambda_h, \lambda_E, \lambda_\phi, \lambda_\gamma)^T$ are the corresponding Lagrange multipliers. The Lagrange multipliers satisfy the adjoint equations

$$\dot{\lambda}_\xi = -\left(\frac{\partial H}{\partial \xi}\right)^T, \quad \lambda_\xi(t_f) = (v_x, v_y, v_h, 0, 0, 0)^T \tag{15}$$

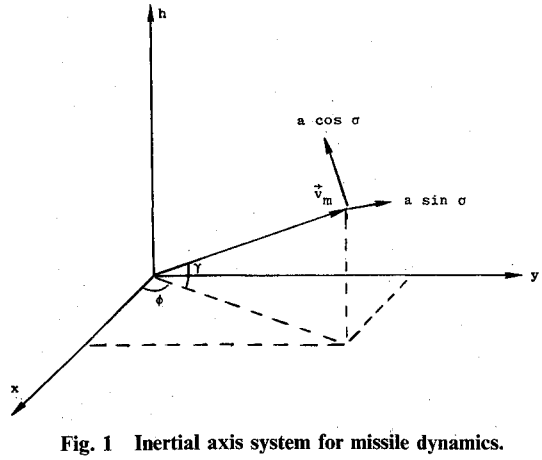

Fig. 1 Inertial axis system for missile dynamics.

Observe that λ_x and λ_y are constant, as H does not depend on x and y. The optimal control solution is determined by the optimality conditions

$$\text{i)} \quad \frac{\partial H}{\partial a} = 0$$

$$\text{ii)} \quad \frac{\partial H}{\partial \sigma} = 0$$

$$\text{iii)} \quad \int_{t_0}^{t_f} \frac{\partial H}{\partial \tau_c} \mathrm{d}t = 0$$

$$\text{iv)} \quad H(t_f) = 0 \tag{16}$$

Condition iii can be obtained by employing the usual first variation arguments on the Hamiltonian[7] and by noting that the coast time τ_c is a parameter. Note further that this condition is distinct from that given by Pontryagin et al. (Ref. 8, theorem 17) for the fixed final time problem with parameters. Condition iv is the transversality condition for a free final time. It may be mentioned here that this time-range optimal problem has been analyzed to a certain extent using reduced-order models in Refs. 9–11.

Simplified Pulse-Motor Ignition Control

To simplify the optimal control problem, the joint optimization problem is transformed into two separate, but coupled, subproblems, respectively, for optimizing the interpulse coast time τ_c (pulse-motor ignition control) and the lift variables a and σ (guidance).

Optimization of the interpulse coast time is considered only between the first and second pulses only. This corresponds to stage II, indicated in Fig. 2. When optimization of τ_c is disassociated from that of a and σ, it is assumed that the guidance can be completely scheduled if τ_c is given. Based on this assumption, the parameter τ_c can be optimized alone.

In the optimization of τ_c, it has been assumed that the complete guidance solution is available if τ_c is known. A near-optimal guidance solution, when τ_c is known, is given in Ref. 1 with a and σ being the control variables. This solution is based on the application of singular-perturbation techniques to the optimal control problem. This suboptimal solution can be used in implementing the τ_c control logic, as well as for determining the desired lift for the guidance law. The actual manner in which the singular-perturbation midcourse guidance is integrated with the pulse-motor ignition control will be discussed in Sec. III.

Now, under the assumption that the other control variables are scheduled optimally, an infinitesimal perturbation in ignition of the second pulse by $\delta\tau_c$ would cause a cost perturbation[7] of

$$\delta J = \left(\int_{t_0}^{t_f} \frac{\partial H}{\partial \tau_c} \mathrm{d}t\right) \delta\tau_c \tag{17}$$

This leads to the optimal relationship of condition iii of Eq. (16), which should be solved for the optimal interpulse coast time; then, if the optimal coast time calls for an ignition time less than or equal to current time t_0, the second pulse would be fired immediately. This method, however, would require the implicit solution of condition iii of Eq. (16) for τ_c, which prohibits a real-time on-board implementable algorithm.

To simplify the formulation further, it is realized that the optimal ignition time can be judged to fall on either side of the nominal value at which Eq. (17) is evaluated. If, in addition, Eq. (17) is evaluated with a nominal delay time corresponding to firing the pulse immediately at time t_0, then it is meaningful to consider only positive values of $\delta\tau_c$. Specifically, if Eq. (17) concludes that a delay in pulse ignition ($\delta\tau_c > 0$) would cause an increase in cost ($\delta J > 0$), then the pulse should be fired immediately. This translates into the following logic: Evaluate

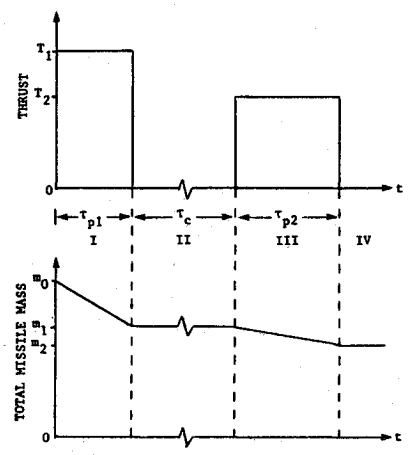

Fig. 2 Simplified thrust and missile mass profiles.

the integral

$$\int_{t_0}^{t_f} \frac{\partial H}{\partial \tau_c}\,\mathrm{d}t$$

with a nominal ignition time at t_0, and fire the pulse immediately if the integral solves out to be positive (i.e., ≥ 0),

The Hamiltonian in Eq. (14) reveals that H depends on τ_c explicitly through thrust T and mass m. Hence the integral can be decomposed into two specific terms by chain rule as follows:

$$\int_{t_0}^{t_f} \frac{\partial H}{\partial \tau_c}\,\mathrm{d}t = \int_{t_0}^{t_f} \left(\frac{\partial H}{\partial T}\frac{\partial T}{\partial \tau_c} + \frac{\partial H}{\partial m}\frac{\partial m}{\partial \tau_c}\right)\mathrm{d}t$$

$$= \int_{t_0}^{t_f} \left(\frac{\lambda_E v}{mg}\frac{\partial T}{\partial \tau_c} - \frac{\lambda_E v(T-D)}{m^2 g}\frac{\partial m}{\partial \tau_c}\right)\mathrm{d}t \qquad (18)$$

where the last equality follows from Eq. (14). For a small nonzero $\delta\tau_c$, the perturbation on the thrust profile is illustrated in Fig. 3. To simplify notations, the variable τ_c can be conveniently redefined to be relative to time zero, so that the nominal value of τ_c is $\tau_c^* = t_0$. This corresponds to a nominal thrust profile of

$$T(t) = T_2[\mathscr{H}(t-\tau_c) - \mathscr{H}(t-\tau_c-\tau_{p2})] \qquad (19)$$

It follows that

$$\left.\frac{\partial T}{\partial \tau_c}\right|_{\tau_c = t_0}(t) = T_2[-\delta(t-\tau_c) + \delta(t-\tau_c-\tau_{p2})]_{\tau_c = t_0}$$

$$= T_2[-\delta(t-t_0) + \delta(t-t_0-\tau_{p2})] \qquad (20)$$

where δ is the Dirac delta distribution. Assuming the specific impulse stays constant through the pulse, the rectangular thrust profile indicates a constant mass-flow rate and the mass profile can be expressed as

$$m(t) = m_1 + \dot{m}(t-\tau_c)\mathscr{H}(t-\tau_c) - \dot{m}(t-\tau_c-\tau_{p2})\mathscr{H}(t-\tau_c-\tau_{p2})$$

where m_1 ($= m_0 - k_1\tau_{p1} > 0$) is the missile mass at first pulse burn-out, and $\dot{m}$ ($= -k_2 < 0$) is the constant mass-flow rate during the second pulse as given in Eq. (12). Then

$$\left.\frac{\partial m}{\partial \tau_c}\right|_{\tau_c = t_0}(t) = \dot{m}[-\mathscr{H}(t-\tau_c) + \mathscr{H}(t-\tau_c-\tau_{p2})]_{\tau_c = t_0}$$

$$= \dot{m}[-\mathscr{H}(t-t_0) + \mathscr{H}(t-t_0-\tau_{p2})] \qquad (21)$$

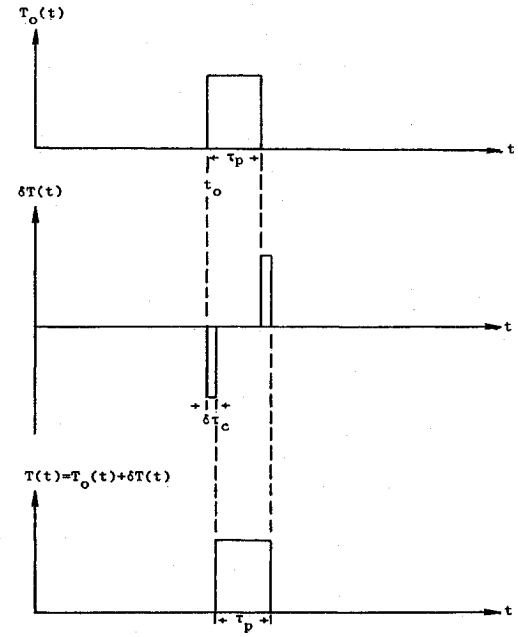

Fig. 3 Perturbation in time of second thrust pulse.

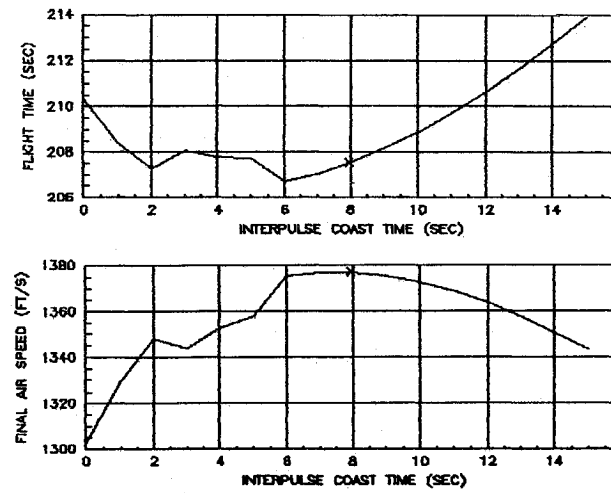

Fig. 4 Pulse-motor ignition control validation: coaltitude stationary target.

The expressions in Eqs. (20) and (21) can be substituted into the integral of Eq. (18), which can then be simplified to

$$\int_{t_0}^{t_f} \frac{\partial H}{\partial \tau_c}\,\mathrm{d}t = \frac{T_2}{g}\left[\frac{\lambda_E(t_0+\tau_{p2})v(t_0+\tau_{p2})}{m(t_0+\tau_{p2})} - \frac{\lambda_E(t_0)v(t_0)}{m(t_0)}\right] + \int_{t_0}^{t_0+\tau_{p2}} \frac{\lambda_E v(T_2-D)\dot{m}}{m^2 g}\,\mathrm{d}t \qquad (22)$$

Pulse-Motor Ignition Control Logic

Fire the pulse immediately if, and only if, the integral in Eq. (22) is positive.

Observe that, to evaluate Eq. (22), the corresponding values of λ_E, v, and m are needed in the interval $[t_0, t_0+\tau_{p2}]$, under the hypothesis that the pulse is fired at t_0. The value of m is predefined in Eq. (12). An approximation procedure for evaluating λ_E and v during the midcourse phase is discussed in the next section.

III. Implementation Algorithm of Pulse-Motor Control and Midcourse Guidance

The pulse-motor ignition control law developed previously dictates that the pulse should be ignited at the current time t_0 if the integral in Eq. (22) solves out to be positive. The integral is evaluated under the following hypothetical conditions:

1) The pulse is ignited at t_0.

2) The guidance command is optimal relative to the same performance index [Eq. (13)] and propulsion information as above.

To evaluate the integral in Eq. (22), it is observed that such quantities as T_2 and m are given, and v can be predicted reasonably accurately in the time interval $[t_0,\ t_0+\tau_{p2}]$. The only other information needed is λ_E in the interval $[t_0, t_0+\tau_{p2}]$, associated with the optimal guidance solution. To achieve a real-time implementable ignition control algorithm, we can determine λ_E in $[t_0, t_0+\tau_{p2}]$ based on the reduced-order guidance solution of Ref. 1.

The outer solution of the guidance problem in Ref. 1 consists of x, y, and E as the state variables. It was established that when the Hamiltonian H is not an explicit function of time, then the adjoint variable λ_E can be determined in closed form. In particular, the Hamiltonian H is generally an explicit function of time through thrust T and mass m; however, if we consider the period after the pulse burns out (i.e., $t > t_0+\tau_{p2}$), then $T=0$ and m is constant, and thus H is no longer an explicit function of time. In this period, the outer solution (denoted by subscript 1) of λ_E can be solved as [see Ref. 1, Eq. (29)].

$$\lambda_{E1}(t) = \frac{mg}{-D_1(t)}\left[\frac{1}{v_1(t_f)} - \frac{1}{v_1(t)}\right], \quad t\in[t_0+\tau_{p1},\ t_f] \quad (23)$$

This expression provides the means to determine $\lambda_E(t_0+\tau_{p2})$, if we can reasonably estimate $v_1(t_f)$. Subsequently, all values of λ_E in the interval $[t_0, t_0+\tau_{p2}]$ can be determined numerically by integrating backwards the differential equation of λ_E as defined in Eq. (15). Assuming the drag coefficient is constant in the period of interest, we can reduce the differential equation to the following form:

$$\dot{\lambda}_E(t) = -\frac{(T_2-3D(t))}{m(t)v(t)}\lambda_E(t) + \frac{g}{v(t)v(t_f)}, \quad t\in[t_0,\ t_0+\tau_{p2}] \quad (24)$$

The crucial task remaining for the implementation of the ignition control logic is a reasonable method for estimating the quantity $v_1(t_f)$. This term is resolved as the final missile speed at the optimal altitude. In the outer solution of the guidance problem, altitude h is treated as a control variable. In the interval $[t_0+\tau_{p2},\ t_f]$, the optimal altitude h_1 is determined implicitly through the term $\partial D/\partial h$ satisfying [see Ref. 1, Eq. (30)]

$$\left.\frac{\partial D}{\partial h}\right|_E (h_1(t)) = -\frac{g v_1(t_f) D_1(t)}{v_1(t)^2[v_1(t)-v_1(t_f)]}, \quad t\in[t_0+\tau_{p2},\ t_f] \quad (25)$$

Since the ignition control law in the procedure described subsequently is evaluated at every sample instant, $v_1(t_f)$ is estimated iteratively by using its existing value to determine h_1 according to Eq. (25), and then $v_1(t_f)$ is updated based on the h_1 solution. This procedure inevitably needs an initial guess of $v_1(t_f)$ to commence. The basic pulse-motor ignition control law is implemented as follows.

Basic Pulse-Motor Ignition Control Algorithm

Step 1. Assume immediate motor firing, estimate speed increase Δv during burn due to thrust and drag.

Step 2. Predict intercept point assuming missile speed is constant as given by

$$v(t_0+\tau_{p2}) = v(t_0) + \Delta v$$

and that the target is travelling at constant velocity.

Step 3.

a) Assume missile altitude can change instantaneously *after* pulse burnout. Determine optimal altitude $\bar{h}_1 = h_1(t_0+\tau_{p2})$ according to

$$\left.\frac{\partial D}{\partial h}\right|_E (\bar{h}_1) = -\frac{g v_1(t_f) D_1(t_0+\tau_{p2})}{v_1(t_0+\tau_{p2})^2[v_1(t_0+\tau_{p2}) - v_1(t_f)]}$$

where $v_1(t_0+\tau_{p2})$ and $D_1(t_0+\tau_{p2})$ are computed iteratively below, and $v_1(t_f)$ is computed iteratively in step 4.

b) Update (iteratively) $v_1(t_0+\tau_{p2})$ by

$$v_1(t_0+\tau_{p2}) = \sqrt{2g\left[h(t_0) + \frac{v(t_0+\tau_{p2})^2}{2g}\right] - \bar{h}_1}$$

c) Update drag $D_1(t_0+\tau_{p2})$ at $\bar{h}_1$ and $v_1(t_0+\tau_{p2})$ (with lift = weight condition from the outer solution).

Step 4. Estimate $v_1(t_f)$ by the following method.

a) Estimate range covered during pulse burn and use it to determine horizontal range left after pulse burn.

b) Find speed of missile at constant altitude $\bar{h}_1$ after covering the necessary horizontal cruise range, call it $\bar{v}_1(t_f)$. (A simple exponential-decay formula is used in the current implementation.)

c) Given the specific energy at that point

$$E(t_f) = \bar{h}_1 + \frac{\bar{v}_1(t_f)^2}{2g}$$

recompute the optimal altitude $h_1(t_f)$ using the same $\partial D/\partial h$ value computed in step 3a above.

d) Update the final missile speed at the new optimal altitude

$$v_1(t_f) = \sqrt{2g[E(t_f) - h_1(t_f)]}$$

Step 5. Compute $\lambda_{E1}(t_0+\tau_{p2})$ using Eq. (23).

Step 6. Determine values of λ_E in the interval $[t_0, t_0+\tau_{p2}]$ by integrating Eq. (24) backwards in time, with m, v, and D updated at each integration step.

Step 7. Evaluate the ignition control law [Eq. (22)] using the quantities determined previously.

The basic algorithm constitutes an approximate method for implementing the reduced-order solution of the pulse-motor ignition control problem. A few constraints and characteristics of the MRAAM mission are not addressed by the basic algorithm, such as minimum missile speed required for controllability and excessive heading angle error. These conditions are resolved by supplementing the basic ignition control algorithm with additional control commands to result in the following algorithm.

Pulse-Motor Ignition Control Algorithm

Data: Minimum missile speed allowed during coast, $v_{\min}$.
Maximum heading error allowed for pulse firing, $\phi_{\max}$.

At each sample instant, carry out the following:

Step 1. If second pulse has already fired, go to step 6.

Step 2. Evaluate basic pulse-motor ignition control algorithm: Command second pulse ignition if integral in Eq. (22) is positive.

Step 3. If missile heading is not within $\phi_{\max}$ of desired missile heading for intercept, command ignition delay.

Step 4. If speed of missile is less than $v_{\min}$, command second pulse ignition.

Step 5. If first pulse has not yet burnt out, command ignition delay.

Step 6. End of algorithm.

Remark: Since the basic ignition control algorithm needs to update the variables $v_1(t_0+\tau_{p2})$, and $v_1(t_f)$ iteratively, execution of the algorithm should be allowed even before the first pulse has burnt out. This is achieved by step 2 of the preceding algorithm.

Remark: The ignition control algorithm is to be used in conjunction with the singular-perturbation midcourse guidance algorithm of Ref. 1; however, the guidance algorithm assumes that propulsion information is available, whereas the ignition control algorithm does not predict ahead of time what τ_c should be. (Even though it hypothesizes immediate firing in its evaluation, the algorithm does not know what τ_c will be if the ignition control law requests a delay in the pulse.) With no knowledge of τ_c available, the actual guidance law would have to assume that τ_c is infinite, i.e., no second pulse will be fired. Consequently, the guidance solution actually used in the guidance law may be different from that used by the pulse motor ignition logic, because the latter hypothesizes immediate firing of the second pulse in its formulation.

IV. Algorithm Validation and Performance Evaluation

The pulse-motor ignition control algorithm in conjunction with the singular-perturbation midcourse guidance have been incorporated into a five-degree-of-freedom (5-DOF) missile simulation of a generic medium-range air-to-air missile.[1] With this simulation we compare the performance of a generic pulse-motor design to that of a baseline boost-sustain motor. For proper evaluation against advanced airborne targets, the target model can command certain pseudointelligent maneuvers including midcourse and final evasive maneuvers. The evasive target maneuver algorithm is the same one used in Ref. 1.

Propulsion Definition

Two solid-propellant rocket motors are defined for the MRAAM mission for comparison: a boost-sustain and a two-pulse motor, of which the former serves as a baseline for evaluation of the pulse motor. The propulsion and mass properties of both motors are of a generic nature, not intended to resemble any existing or anticipated motor designs. The external configuration of both motors are assumed to be identical, which is simulated with the same aerodynamic model of the generic BVR missile of Ref. 1.

Performance data of the pulse motor is summarized in Table 1. The missile has a launch mass of about 340 lb. Propellant mass is assumed to be about 100 lb. The boost-sustain motor has similar properties as the generic model used in Ref. 1, except that the amount of propellant has been scaled to equal that of the pulse motor. The pulse motor is slightly heavier than the boost-sustain motor, due to the additional thermal barrier that would be expended upon ignition of the second pulse and additional igniter hardware. Although the performance data are assumed at 77°F, sea level, they are used in the evaluation below without altitude correction due to atmospheric pressure variation. This simplification slightly favors the pulse motor.

Guidance Laws

During the homing phase, the MRAAM studied here uses a linear optimal guidance law, which is an extension of the guidance law of Ref. 12 that also utilizes available target acceleration information. Using the same terminal guidance for both motors assures that any performance difference is a consequence of the motor configuration and midcourse guidance.

Table 1 Motor performance data

Missile launch mass, lbm	341.9
Propellant mass, lbm (includes thermal barrier for pulse motor)	103.6
Pulse split, % in propellant	50/50
Specific impulse, lbf-s/lbm	247
Action time, s	2.5/3
Thrust, lbf	5120/4267
Total impulse, lbf-s	25,600

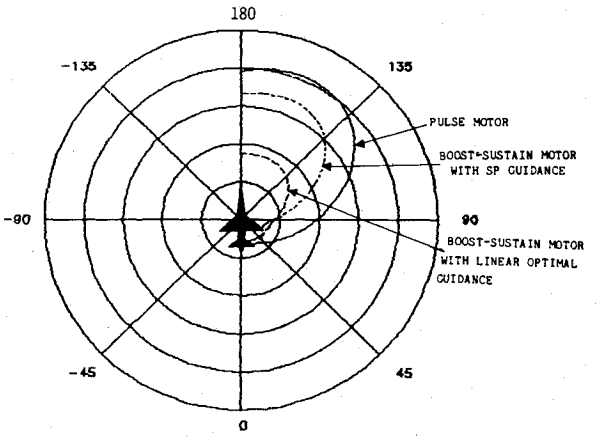

Fig. 5a Coaltitude outer launch boundary.

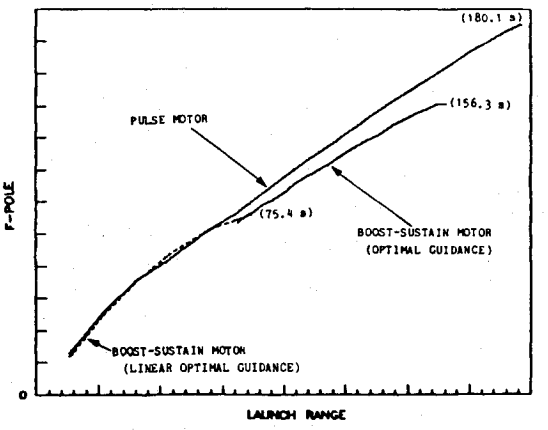

Fig. 5b f-pole profiles in head-on direction.

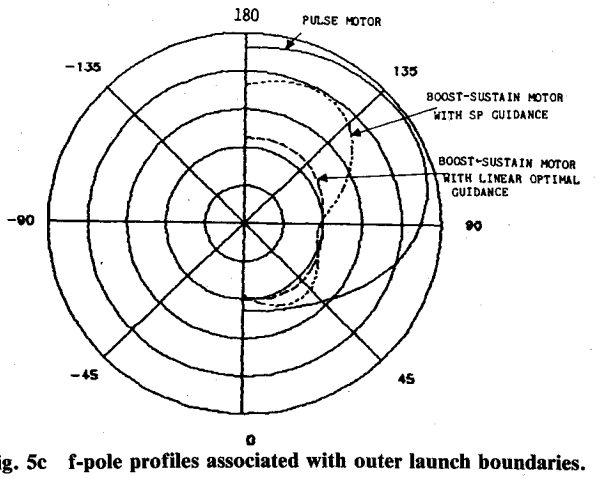

Fig. 5c f-pole profiles associated with outer launch boundaries.

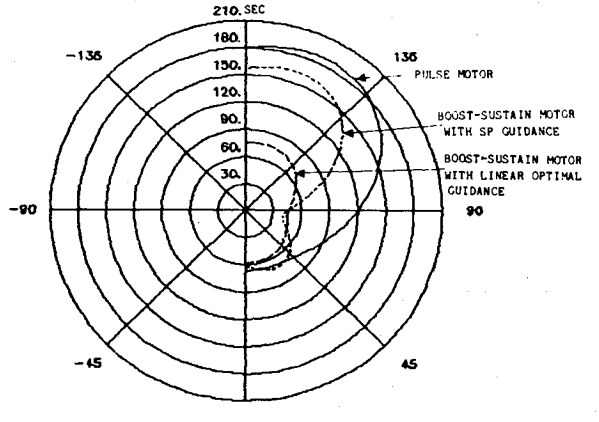

Fig. 5d Flight-time profiles associated with outer launch boundaries.

During midcourse, the pulse motor is always used in conjunction with the pulse-motor ignition control algorithm of this paper and the singular-perturbation (SP) midcourse guidance of Ref. 1. The boost-sustain motor, on the other hand, can use either the SP guidance or the linear-optimal homing guidance plus a prescribed vertical g-bias command during midcourse. The latter guidance is the baseline guidance of Ref. 1.

Validation of Pulse-Motor Ignition Control

An important issue of the pulse-motor ignition control algorithm is whether it commands pulse-motor ignition close to the optimal ignition instant. We investigate this problem by comparing the performance of the algorithm to that established by a parametric scan of different interpulse coast times. To assure that no performance discontinuities would be caused by the adaptive target maneuver, a stationary target is used in this evaluation. Specifically, the missile is launched at 20,000 ft altitude with an initial speed of 307 ms^{-1}, at a stationary target at the same altitude and near the outer launch boundary range. Figure 4 depicts the resulting flight times and terminal airspeeds from the parametric scan. The cross ($\times$) indicates the ignition time selected by the pulse-motor ignition control algorithm. It is observed that for coast times less than 6 s, the performance is erratic with varying coast time. Even though there exists a locally minimum flight time at a pulse delay of 2 s, the ignition control does not command ignition until about 8 s, in a region where performance in variation with coast time is more systematic. Furthermore, the flight time is less than 1 s above the actual minimum, whereas the terminal speed attains a maximum value. It is interesting that the terminal speed maximization feature of the near-optimal pulse-motor ignition control is reminiscent of the long-range aircraft pursuit-evasion problem wherein the interceptor attempts to stay at the maximum speed point on its level flight envelope.[9,11] We conclude that the ignition control algorithm indeed commands motor ignition within the most desirable instant.

Performance Evaluation

The most important measures of effectiveness for the MRAAM mission are the effective outer launch boundary (OLB) and f-pole, which is related to the time of flight. These measures are adopted here to compare the performance of the two motors. The engagement scenario is representational of fighter intercepts, with missile launched at 20,000 ft altitude and 307 ms^{-1} speed against a coaltitude target. The target is assumed to be traveling at a constant speed of 307 ms^{-1}, with $2g$ of swerving midcourse maneuver and $6g$ of maximum maneuver capability employed within a range of 2 km.

Three motor/guidance combinations are evaluated. The baseline uses the boost-sustain motor with the g-biased linear optimal guidance. The pulse motor uses the ignition control algorithm and SP midcourse guidance. To separate the performance improvement due to the pulse motor from that due to the SP guidance, we have included a third combination, which uses the boost-sustain motor with the SP guidance.

The respective outer launch boundaries of the three cases are illustrated in Fig. 5a. The polar plot is target-centered with aspect angles indicated around the perimeter. It should be pointed out that the boundaries are obtained with five data points, at multiples of 45 deg aspect angle. The performance in between these data points is fitted using cubic splines and, therefore, does not represent true simulation results. This is, in fact, why the boost-sustain motor with SP guidance seems to have a diminished launch boundary than the baseline between 45 and 90 deg aspect. MRAAM's are most typically used in a head-on situation and, in this case, the pulse motor produces about 125% improvement in OLB over the baseline. It can be seen that about 70% of the improvement is attributed to the SP guidance law, and the rest is due to the pulse motor with the ignition control algorithm.

Figure 5b compares the f-pole obtained for launches with head-on aspects. It is observed that the pulse motor experiences some f-pole improvement over the baseline motor under some conditions. However, when maximum achievable f-pole is compared, the pulse motor displays around 100% improvement over the baseline, due to the extra f-pole associated with the expanded outer launch boundary. The figure also shows that the SP guidance can contribute about one-half of the performance improvements achievable by the pulse motor with SP guidance and control. The rest of the improvement can be accounted for only by the additional energy management flexibility of the pulse motor through pulse delays. The quantities expressed in parentheses in the figure represent the time of flight associated with the corresponding outer launch range. Figures 5c and 5d show, respectively, the f-pole and flight-time profiles associated with the outer launch boundaries. It is obvious that the pulse motor leads to increased f-poles associated with longer launch ranges over the baseline in all aspect angles. There may be, however, other conceivable constraints that would prevent the pulse motor from fully achieving such potential improvements; for instance, the current production technology of on-board batteries would prohibit the longer flight time associated with the longer-range launches.

Flyout Example

We continue comparison between the pulse motor and the baseline boost-sustain motor with a flyout simulation. The missile with either motor is launched outside the launch boundary of the boost-sustain motor in a head-on scenario, at the same coaltitude condition as above. Both motors are evaluated with

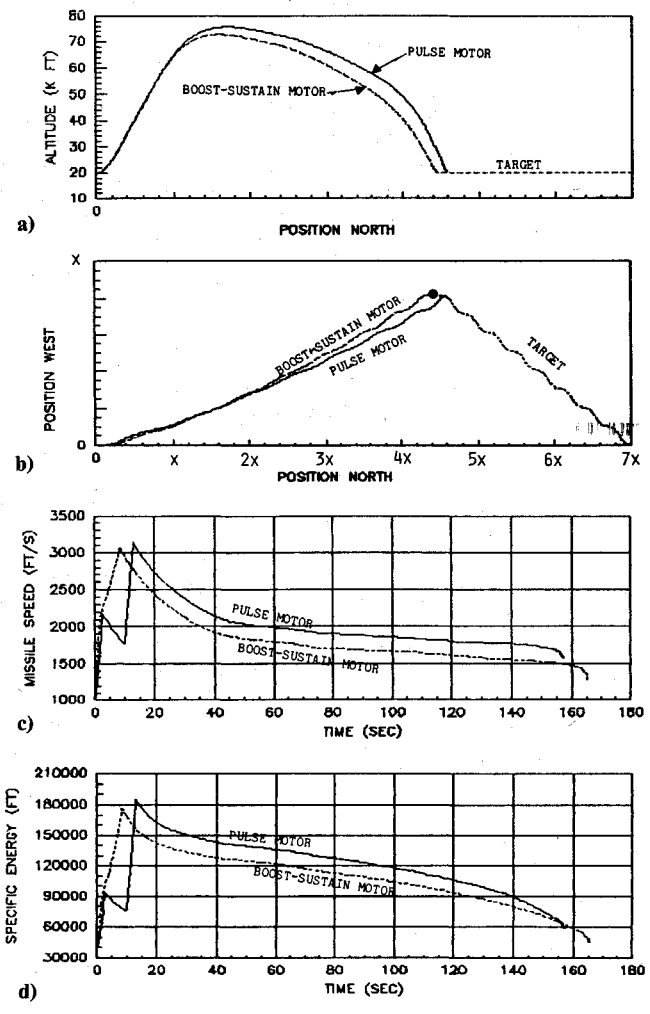

Fig. 6 Flyout example: a) vertical trajectory; b) horizontal trajectory; c) missile speed profile; d) specific energy profile.

Table 2 Final results for flyout comparison

	Pulse motor	Boost-sustain motor
Interpulse coast time, s	7.4	—
Flight time, s	157.1	165.5
Miss distance, ft	2.9	27.5
Final speed, ft-s^{-1}	1576	1262

the singular-perturbation midcourse guidance. The trajectories are compared in Fig. 6, and the final results are summarized in Table 2.

With a miss distance requirement of 10 ft for successful intercept, Table 2 indicates that the pulse motor scores a successful hit while the boost-sustain motor misses. In addition, the pulse motor also delivers a higher final airspeed with a shorter flight time.

The flight trajectories of Figs. 6a and 6b establish that the pulse motor flies at a higher optimal altitude and intercepts the head-on target earlier (i.e., further down range). The higher optimal altitude is a direct consequence of higher available energy, which is evident in Figs. 6c and 6d. Pulse motors, due to improved specific impulse, generally have 5–7% more total impulse than boost-sustain motors. The airspeed profiles in Fig. 6c show that the incremental speed improvement of the pulse motor during the second pulse far exceeds the total-impulse advantage margin. Most of the speed improvement is attributed to a lower accumulated drag effect encountered during the second pulse burn. The lower accumulated drag effect is a result of

1) lower missile speed at ignition, which leads to lower dynamic pressure and hence lower drag;

2) higher altitude at ignition, which also leads to lower dynamic pressure (the second pulse of the pulse motor ignites at about 28,000 ft whereas the sustain motor ignites near 20,000 ft);

3) shorter burn time of the pulse motor, which reduces proportionally the accumulated drag effect during burn.

V. Conclusions

A reduced-order, near-optimal, pulse-motor ignition control logic has been derived and verified for use in conjunction with singular-perturbation optimal guidance algorithms. Given that the singular-perturbation guidance is used, the ignition logic yields pulse firing times very close to those that maximize terminal airspeed of the missile while providing flight times within 1% of the minimum realizable flight time; this result is provided consistently, regardless of the launch conditions or target behavior in the interval between launch and the second pulse firing.

Use of a pulse motor with the same amount of propellant in place of a boost-sustain motor, both in conjunction with the singular-perturbation guidance, increased the 20 k-ft coaltitude outer launch boundary of the medium-range missiles by amounts that range from 10 to 100% depending upon launch aspect; the least improvement was obtained with head-on and tail-on launches, whereas 100% improvement was realized for crossing targets. Head-on-launch f-pole values were increased nearly 28% for the coaltitude launch condition.

The near-optimal ignition logic provides the most in performance benefits for engagements carried out against targets at low-to-moderate altitudes. With increasing target and launch altitude, an anticipated degradation in the advantage observed for pulse motors occurs because of the reduced impact of aerodynamic forces on performance and correspondingly less payoff from energy management strategies. When the launch and target altitudes are above 50,000 ft, the performance advantage of a pulse motor over a boost-sustain motor reduces to slightly more than the few percent difference in vacuum total impulse.

Acknowledgments

This work was supported by the Air Force Rocket Propulsion Laboratory, Edwards AFB, CA, under Contract F04611-82-0035.

References

[1]Cheng, V. H. L. and Gupta, N. K., "Advanced Midcourse Guidance for Air-to-Air Missiles," *Journal of Guidance, Control and Dynamics*, Vol. 9, March-April 1986, pp. 135–142.

[2]Sridhar, B. and Gupta, N. K., "Missile Guidance Laws Based on Singular Perturbations Methodology," *Journal of Guidance and Control*, Vol. 3, March-April 1980, pp. 158–165.

[3]Calise, A. J., "Singular Perturbation Techniques for On-Line Optimal Flight Path Control," *Journal of Guidance and Control*, Vol. 4, July-Aug. 1981, pp. 398–405.

[4]Price, D. B., Calise, A. J., and Moerder, D. D., "Piloted Simulation of an Onboard Trajectory Optimization Algorithm," *Journal of Guidance, Control and Dynamics*, Vol. 7, May-June 1984, pp. 355–360.

[5]Isaacs, R. P., *Differential Games*, Robert E. Krieger Publishing Co., New York, 1975.

[6]Cheng, V. H. L. and Briggs, M. M., "Strap-Down Seeker Advanced Guidance," Final Report prepared for Air Force Armament Laboratory, Eglin AFB, FL, under Contract F08635-82-C-0305, Sept. 1984.

[7]Bryson, A. E. and Ho, Y. C., *Applied Optimal Control*, Blaisdell, Waltham, MA, 1969.

[8]Pontryagin, L. S., Boltyanskii, V. A., Gamkrelidze, R. V., and Mishchenko, E. F., *The Mathematical Theory of Optimal Processes*, John Wiley, New York, 1962.

[9]Kelley, H. J., "Aircraft Maneuver Optimization by Reduced Order Approximation," *Control and Dynamic Systems*, Vol. 10, edited by C. T. Leondes, Academic Press, New York, 1973, pp. 131–178.

[10]Menon, P. K. A., "Optimal Symmetric Flight with an Intermediate Vehicle Model," Ph.D. dissertation, VPI & SU, Blacksburg, VA, Sept. 1983.

[11]Weston, A. R., "On-Board Near-Optimal Climb-Dash Energy Management," Ph.D. dissertation, VPI & SU, Blacksburg, VA, Dec. 1982.

[12]Vergez, P. L., "Linear Optimal Guidance for an AIM-9L Missile," *Journal of Guidance and Control*, Vol. 4, Nov.-Dec. 1981, pp. 662–663.